RSC Medicinal Chemistry

ROYAL SOCIETY OF CHEMISTRY

RESEARCH ARTICLE

View Article Online
View Journal | View Issue

Check for updates

Cite this: *RSC Med. Chem.*, 2024, **15**, 2400

N-Sulfonylphenoxazines as neuronal calcium ion channel blockers†

Matthieu Schmit,[ab] Md. Mahadhi Hasan,‡[c] Yashad Dongol,[c] Fernanda C. Cardoso,[c] Michael J. Kuiper,[d] Richard J. Lewis,[c] Peter J. Duggan *[be] and Kellie L. Tuck *[a]

Neuropathic pain is a type of chronic pain, usually caused by nerve damage, that responds poorly to traditional pain therapies. The N-type calcium channel ($Ca_V2.2$) is a well-validated pharmacological target to treat this condition. In order to further improve the inhibition of the N-type calcium channel relative to previously described inhibitors, and also address their problematic instability in blood plasma, the development of *N*-sulfonylphenoxazines as new calcium channel inhibitors was pursued. A series of *N*-sulfonylphenoxazines bearing ammonium side chains were synthesised and tested for their ability to inhibit both $Ca_V2.2$ and $Ca_V3.2$ (T-type) neuronal ion channels. Compounds with low micromolar activity in $Ca_V2.2$ were identified, equivalent to the most effective reported for this class of bioactive, and calculations based on their physical and chemical characteristics suggest that the best performing compounds have a high likelihood of being able to penetrate the blood–brain barrier. Representative *N*-sulfonylphenoxazines were tested for their stability in rat plasma and were found to be much more resilient than the previously reported *N*-acyl analogues. These compounds were also found to be relatively stable in an *in vitro* liver microsome metabolism model, the first time that this has been investigated for this class of compound. Finally, molecular modelling of the $Ca_V2.2$ channel was used to gain an understanding of the mode of action of these inhibitors at a molecular level. They appear to bind in a part of the channel, in and above its selectivity filter, in a way that hinders its ability to undergo the conformational changes required to open and allow calcium ions to pass through.

Received 9th May 2024,
Accepted 9th June 2024

DOI: 10.1039/d4md00336e

rsc.li/medchem

Open Access Article. Published on 12 June 2024. Downloaded on 2/3/2026 11:10:36 AM.
This article is licensed under a Creative Commons Attribution-NonCommercial 3.0 Unported Licence.

Introduction

Neuropathic pain is a condition stemming from nerve damage caused by surgery, trauma, infection or disease, which results in pain, most often chronic, even in the absence of stimuli. The prevalence of severe neuropathic pain in the general population has been estimated to be as high as 5%.[1] The most commonly studied types of neuropathic pain in clinical trials include peripheral diabetic neuropathy, which is caused by chronically high blood glucose levels damaging nerves and affecting up to 70% of type 2 diabetics; postherpetic neuralgia, a complication encountered in up to 20% of varicella zoster virus infections; and neuropathic cancer pain, which is attributable to nerve damage caused by the cancer itself, therapy or surgery. Other occurrences of neuropathic pain include phantom limb pain, post-stroke pain, and as a result of multiple sclerosis or spinal cord injury.[2–4]

Neuropathic pain does not respond well to traditional pain management therapies that employ non-steroidal anti-inflammatory drugs (NSAIDs) such as aspirin or ibuprofen; in about half of the cases, only 30 to 50% pain relief is achieved. Safe and effective therapies are lacking. First line treatments typically rely on antidepressants or anticonvulsant drugs used outside of their initial indication,[5] while in more severe cases opioids are employed.[4,6,7] In recent decades, voltage-gated calcium channels (VGCC), in particular the N-type ($Ca_V2.2$) and T-type ($Ca_V3.1$, 3.2 and 3.3) subtypes, have emerged as promising and valid targets and have become a major focus of research into the treatment of neuropathic pain.[8,9] These

[a] *School of Chemistry, Monash University, Victoria 3800, Australia. E-mail: Kellie.Tuck@monash.edu*
[b] *CSIRO Manufacturing, Research Way, Clayton, Victoria 3168, Australia. E-mail: Peter.Duggan@csiro.au*
[c] *Institute for Molecular Bioscience, The University of Queensland, St. Lucia, QLD 4072, Australia*
[d] *CSIRO Data 61, Clunies Ross Street, Acton ACT 2601, Australia*
[e] *College of Science and Engineering, Flinders University, Adelaide, South Australia 5042, Australia*

† Electronic supplementary information (ESI) available: Synthesis of **2**, NMR spectra, rat plasma stability and liver microsomal stability studies. See DOI: https://doi.org/10.1039/d4md00336e

‡ Current address: Pharmacy Discipline, Life Science School, Khulna University, Khulna, 9208, Bangladesh.

This journal is © The Royal Society of Chemistry 2024

Open Access Article. Published on 12 June 2024. Downloaded on 2/3/2026 11:10:36 AM. This article is licensed under a Creative Commons Attribution-NonCommercial 3.0 Unported Licence.

channels are expressed by cells involved in the transmission of action potentials characteristic of neuropathic pain; thus it is hypothesised that these inhibitors owe their pain blocking effect to shutting down such signals.[10] While there are many new inhibitors undergoing clinical trials, there are currently only three drugs targeting VGCCs approved by the United States Food and Drug Administration for the treatment of neuropathic pain – gabapentin, pregabalin and ziconotide. Gabapentin and pregabalin are small amino acids, initially designed as gamma-amino butyrate (GABA) analogues for the treatment of epilepsy, and have limited effectiveness. Ziconotide, on the other hand, is a synthetic version of the peptide ω-conotoxin MVIIA found in the venom of the marine snail *Conus magus* and is a selective inhibitor of $Ca_V2.2$ channels. Treatment with ziconotide requires that it is injected intrathecally into the spinal fluid of the patient. While it was shown to deliver superior pain relief to that provided by morphine, with no addictive symptoms, the severe side effects and the invasive mode of administration makes ziconotide a less than ideal drug.[8]

Two molecules currently undergoing clinical trials are PP353 (Phase 1b, Persica Pharmaceuticals), an antibiotic formulation for treating chronic lower back pain,[11] and STA363 (Phase 2b, Stayble Therapeutics), aimed at treating pain from herniated discs.[12] The structures of both molecules are currently not in the public domain.

The present study stemmed from a series of iterations beginning with mimics of ω-conotoxin GVIA and proceeding towards smaller, open chain aromatic compounds,[13] and then more constrained analogues, from which the acylphenoxazines **1a–1d** (Fig. 1) were obtained.[14] These compounds showed promising channel-blocking activity relative to positive controls, and in the case of **1b–1d**, favourable central nervous system multiparameter optimisation (CNS MPO)[15,16] scores. However, **1d** in particular was found to be quite unstable in rat plasma, readily undergoing diacylation, and hence making these acyl derivatives unsuitable for further development. In a recently published study, a similar instability in open chain phenoxyanilides was overcome through the substitution of the amide with a more robust sulfonamide link. Interestingly, this was also associated with a marked improvement in the functional inhibition of the target $Ca_V2.2$ ion channel.[17] In the current work, the acyl link in the acylphenoxazines **1b–1d** was substituted for a sulfonyl moiety in a similar way. In addition, the importance of the nature of the side chain on channel blocking activity was further explored with an expanded set of terminal amines, and for the first time, an *in silico* model based on a recently reported $Ca_V2.2$ Cryo-EM structure[18] was used to rationalise the observed results obtained with this class of compound. Finally, the stability of significant compounds in *in vitro* plasma and liver microsome assays was also assessed.

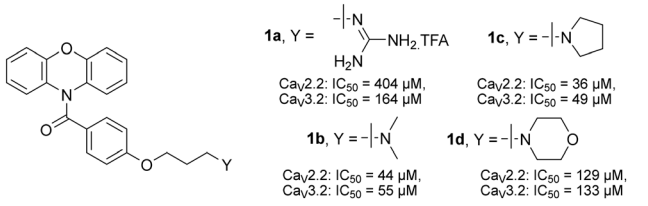

Fig. 1 Chemical structures and ion channel inhibition activity, determined by calcium influx fluorescence imaging assays, of previously reported[14] acylphenoxazines **1a–1d**.

Results and discussion

Chemistry

The first set of sulfonylphenoxazines to be prepared had the side chain linked *via* an aryl ether, analogous to **1a–1d**, and were synthesised in three steps from 4-(3-chloropropoxy) benzenesulfonyl chloride (**2**, see ESI†), as described in Scheme 1. Sulfonylation of phenoxazine with **2**, was readily achieved in pyridine to yield the chloride **3** and a microwave-assisted Finkelstein reaction was subsequently used to prepare an iodide precursor. Treatment of the iodide with six different amines gave compounds **4a–4f** as mono-TFA salts following RP-HPLC purification.

A series of sulfonylphenoxazines was also prepared where the oxygen link to the sidechain was replaced with a nitrogen, as described in Scheme 2. Sulfonylation of phenoxazine was again readily achieved in pyridine, this time with *p*-nitrosulfonyl chloride (**5**), to yield the nitro compound **6**. Hydrogenation gave the aniline **7**, which was acylated with 3-chloropropionyl chloride to give the amide **8**. Borane reduction yielded the substituted aniline **9**, which was converted to a series of diamines (**10a–10f**) in a one-pot Finkelstein reaction followed by alkylation of the appropriate amine. The *N*-methylated aniline **12** was prepared *via* a reductive amination to give **11**, which was used to alkylate dimethylamine. Reductive amination of the aniline **7** with Boc-protected piperidone gave the Boc-protected piperidine **13**, which was deprotected the give the free amine **14**. All final compounds (**10a–10f**, **12** and **14**) were purified by RP-HPLC and obtained as di-TFA salts.

A methoxy analogue of the amines **4a–4f** was also prepared in order to gauge the importance of the terminal amine on $Ca_V2.2$ binding affinity. The methoxy compound (**15**) was prepared from **3** *via* a one-pot Finkelstein reaction followed a substitution reaction with methoxide (Scheme 3). Under the conditions of the reaction **15** was produced as a 1 : 1 mixture with the corresponding allyl ether, which resulted from an elimination reaction, with the two products readily separated using a combination of normal and reversed phase chromatography.

Calcium ion channel inhibition studies

The ability of the sulfonylphenoxazines (**4a–4f**, **10a–10f**, **12**, **14** and **15**) to inhibit functional $h$$Ca_V2.2$ channels was assessed with a calcium flux imaging assay with human neuroblastoma SH-SY5Y cells, as previously described.[5,14,17] The assays were performed in the presence of the Ca_V1 blocker nifedipine and cilnidipine was used as a positive control. The determined IC_{50} values for **4a–4f**, **10a–10f**, **12**

Open Access Article. Published on 12 June 2024. Downloaded on 2/3/2026 11:10:36 AM.
This article is licensed under a Creative Commons Attribution-NonCommercial 3.0 Unported Licence.

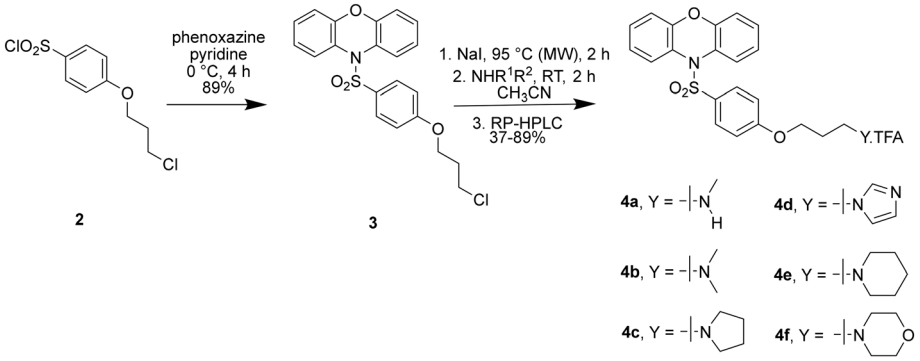

Scheme 1 Synthesis of sulfonylphenoxazine analogues **4a**–**4f**.

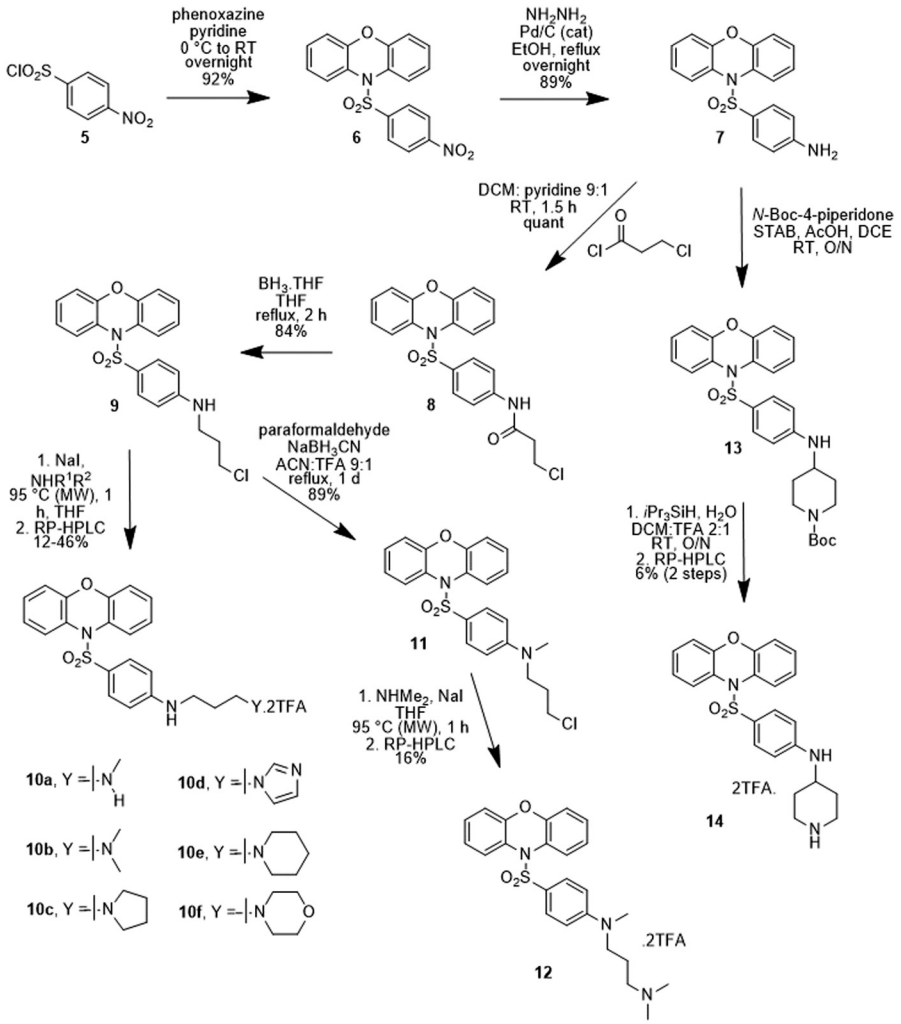

Scheme 2 Synthesis of sulfonylphenoxazine analogues **10a**–**10f**, **12** and **14**.

and **14**, together with those previously reported for compounds **1a**–**1d** and **16** (Fig. 2), are shown in Table 1. Good quality data was obtained for the new compounds, with the measured inhibition for the most active compounds showing narrow errors and confidence intervals. Noteworthy is the observation that the activity for compounds **4a**, **4b** and **10c** is equivalent to the best so far recorded for this class of compound in this $h\mathrm{Ca_V}2.2$ assay. As was observed with the previously reported open chain sulfonylamides (*e.g.* compound **16**),[17] substitution of the acyl functionality for a sulfonyl link has led to a marked improvement in activity (for example the previously reported results for acyl compounds

 This journal is © The Royal Society of Chemistry 2024

Open Access Article. Published on 12 June 2024. Downloaded on 2/3/2026 11:10:36 AM.
This article is licensed under a Creative Commons Attribution-NonCommercial 3.0 Unported Licence.

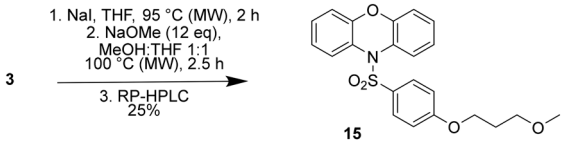

Scheme 3 Synthesis of sulfonylphenoxazine analogue **15**.

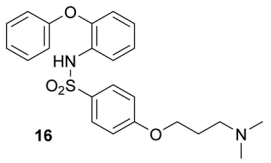

Fig. 2 Chemical structure and ion channel inhibition activity, determined by calcium influx fluorescence imaging assays, of recently reported[17] open chain sulfonylamide **16**.

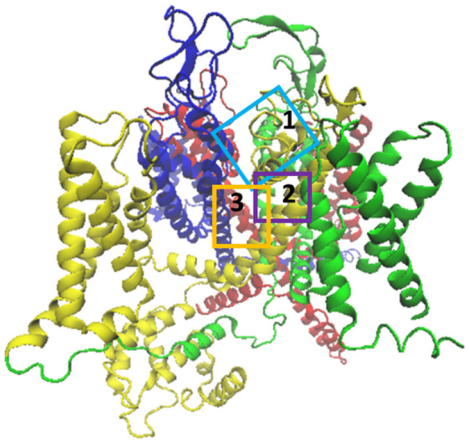

Fig. 3 Side view of the α1 subunit of the $Ca_V2.2$ Cryo-EM structure.[18] Domains I to IV are represented in blue, red, green and yellow respectively. The approximate boundaries of docking sites 1, 2 and 3 are designated in light blue, purple and orange rectangles respectively.

1b–d with those of the corresponding sulfonyl compounds **4b**, **4c** and **4f**), with dimethylamine **4b** showing >10-fold improvement *cf.* **1b.** It was hoped that the replacement of the ether linker with an amine in compounds **10a–10f**, **12** and **14** would provide further hydrogen bonding opportunities in the $Ca_V2.2$ binding site occupied by these compounds (see below) and hence even stronger inhibition, but in most cases no great improvement in activity was seen, with only the imidazole **10d** showing just less than a 4-fold improvement (*cf.* **4d**). The importance of the terminal amine was, however, demonstrated by the marked drop off in affinity shown by the methoxy compound **15** compared to all the corresponding sulfonylphenoxazines **4a–4f.** The majority the sulfonylphenoxazines were also tested for their ability to inhibit $Ca_V3.2$ channels recombinantly expressed in HEK293T cells using a similar calcium flux imaging assay,[14,17] but no strong inhibition was observed, with their measured IC_{50} values all falling in the 40–70 μM range (data not shown), and revealing only weak structure–activity correlations.

Table 1 Functional inhibition of the calcium channels *h*$Ca_V2.2$ by sulfonylphenoxazines **4a–4f**, **10a–10f**, **12**, **14** and **15** and control cilnidipine. Data are presented as mean ± SEM and 95% confidence intervals from *n* = 3 independent experiments

Compound	IC_{50} (μM)	SEM	95% CI (μM)
Cilnidipine	26	4	9–43
1a[a]	404	39	250–650
1b[a]	44	2	35–55
1c[a]	36	2	28–44
1d[a]	129	6	103–161
4a	4.6	0.6	3.8–5.3
4b	4.3	0.6	3.6–5.0
4c	8.0	1.0	6.7–9.3
4d	48.7	3.2	44.4–53.0
4e	7.6	1.1	6.1–9.1
4f	29.0	2.5	25.7–32.3
10a	10.9	1.6	7.4–14.4
10b	9.1	1.0	6.5–11.6
10c	4.4	0.5	3.2–5.6
10d	13.7	1.7	8.3–19.1
10e	15.2	2.1	10.4–20.0
10f	20.8	1.6	15.4–26.2
12	18.7	3.6	13.8–23.6
14	19.9	2.4	16.6–23.2
15	172	21	144–199
16[b]	5.5	0.8	4.9-6.1

[a] From ref. 14. [b] From ref 17.

Molecular modelling

In order to gain a better understanding of how this class of $Ca_V2.2$ channel inhibitors exert their blocking effect, a computational study was undertaken. Previously, three main binding sites for calcium channel inhibitors that occur above the channel's selectivity filter were identified.[5] In Fig. 3 these are designated as binding sites 1, 2 and 3 on a representation of the deactivated cryo-EM structure of $Ca_V2.2$ reported by Gao *et al.* (PDB:7MIY).[18] Site 1, formed around the $S5\text{-}P1_{III}$, $P2_{III}$ and $P2_{IV}$ segments,§ is where ω-conotoxin MVIIA was determined to bind by Gao *et al.*[18] Site 2, consisting of the pocket between the $S5_{III}$, $S6_{III}$ and $S6_{IV}$ segments, is analogous to the dihydropyridine binding site in $Ca_V1.1$ (ref. 19) and is where amitriptyline, maprotiline and other tricyclic antidepressants were predicted to bind in $Ca_V2.2$.[5] Site 3, located above the $S6_I$, $S6_{II}$, $S6_{III}$ and $S6_{IV}$ segments, is analogous to the diltiazem binding site in $Ca_V1.1$ (ref. 19) and is where desipramine and opipramol were predicted to bind in $Ca_V2.2$.[5]

A rigid docking study was undertaken in an attempt to identify the most likely binding sites for the *N*-sulfonylphenoxazines in the $Ca_V2.2$ channel and to understand better the origins of the observed trends in inhibition values. The cryo-EM structure of the channel, determined by Gao *et al.*,[18] was

§ The abbreviations used to identify the various segments and loops in the $Ca_V2.2$ protein structure are defined in a previous publication.[5]

Open Access Article. Published on 12 June 2024. Downloaded on 2/3/2026 11:10:36 AM.
This article is licensed under a Creative Commons Attribution-NonCommercial 3.0 Unported Licence.

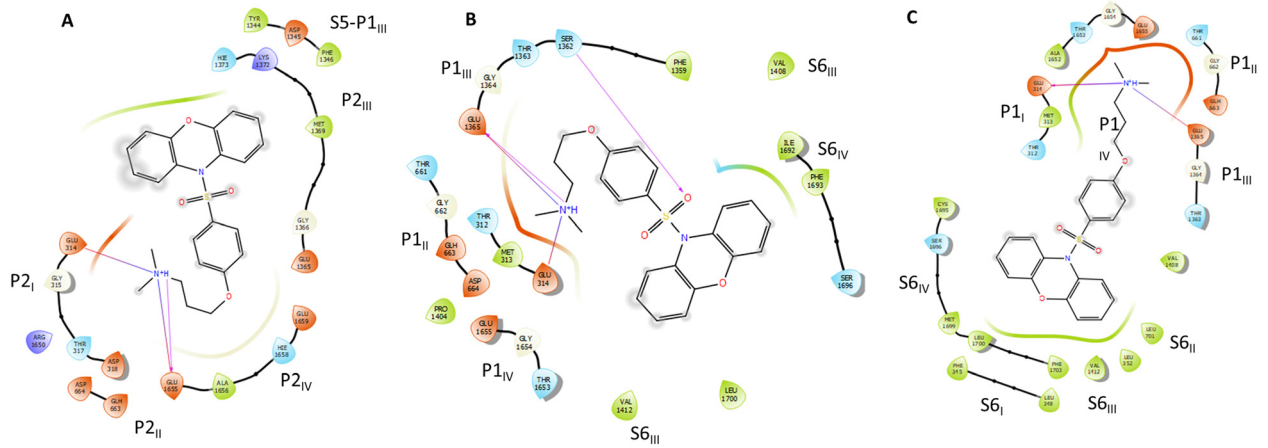

Fig. 4 Ligand interaction diagrams of protonated **4b** in docking site 1 (**A**), docking site 2 (**B**), and docking site 3 (**C**).

imported into Schrödinger Maestro®[20] and the compounds prepared in this study were then rigidly docked into the three sites designated in Fig. 3. There was no observed correlation between the docking scores obtained and experimentally determined inhibition values, but the docking scores obtained for sites 2 and 3 were consistently more favourable than those for site 1.

Images of the results obtained with the dimethylamine (**4b**) docked into the three binding sites are shown in Fig. 4 and S1.† Consistent with the results of the modelling studies of the binding of tricyclic antidepressants (TCAs) to $Ca_V2.2$,[5] all three poses show salt-bridge and hydrogen bond interactions between the ammonium tail and the glutamate residues of the selectivity filter. Similar interactions are not possible with the methoxy analogue (**15**), which experimentally was found to be a two orders of magnitude weaker inhibitor than its amine analogue (**4a**), emphasising that the ability of the ammonium tails of these compounds to bind to the $Ca_V2.2$ selectivity filter appears to be a critical feature of their inhibition effect. The phenoxazine head group of the compounds in this study was found to be coordinated to S6 segments, which together form the internal gate of the channel. It has previously been hypothesised that close coordination of small molecule inhibitors with the S6 segments of the protein structure prevents these segments from efficiently moving away from each other when the channel opens, as having the drug desorb would be thermodynamically unfavourable.[5,19] This may also explain why MONIRO-1, an earlier analogue of the compounds studied here, was found to be a state-dependent inhibitor of $Ca_V2.2$ with a higher affinity for the inactivated state,[21] in which the internal gate is closed. It is not clear why MONIRO-1 would be state-dependent if it bound to $Ca_V2.2$ in docking site 1, as the P2 segments are not known to undergo conformational shifts during channel activation, unlike the S6 segments.[22,23] Coordination of the phenoxazine head group of the compounds in this study to S6 segments may also explain the relatively low but significant residual activity of **15** (IC_{50}: 172 μM). While this compound lacks the ammonium tail group to disrupt the selectivity filter, it would be able interact with the S6 segments in the same way as **4b** and the other phenoxazine analogues appear to do. Therefore, most factors seem to indicate that docking sites 2 and 3 are more likely than docking site 1 to be the actual binding site of the phenoxazine compounds developed.

The substitution of the acyl link to the phenoxazine unit with a sulfonyl attachment resulted in an order of magnitude improvement in potency (compare IC_{50}s for **1b–1d** with **4b**, **4c** and **4f**) and when **4b** was docked into binding site 2 an interaction with the sulfonamide oxygens was observed. In this case Ser1362 was seen to form a hydrogen bond with one of the sulfonamide oxygens. While this was not evident with all of the sulfonylphenoxazines examined, when docked into binding site 2 (Fig. 5), the sulfonamide group was consistently found to be within 3 Å of hydrogen donor residues – either Ser1362, Thr1363 and/or Ser1696. No such association was found when the phenoxazines were docked into site 3. Based on these findings, it appears that the

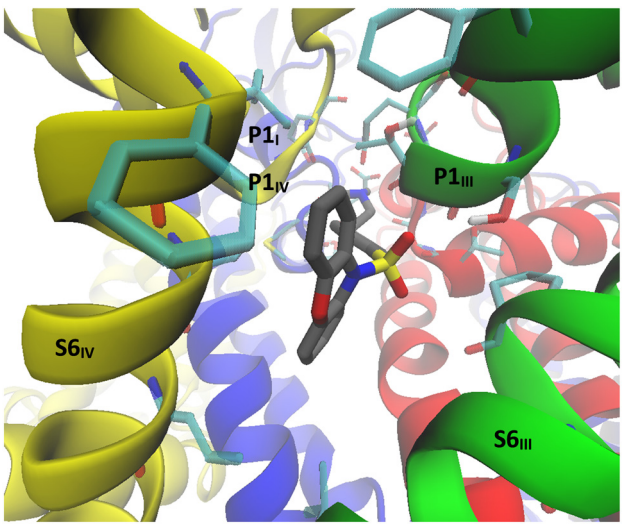

Fig. 5 Diagram of protonated **4b** docked into docking site 2 of the $Ca_V2.2$ Cryo-EM structure.

 This journal is © The Royal Society of Chemistry 2024

Open Access Article. Published on 12 June 2024. Downloaded on 2/3/2026 11:10:36 AM. This article is licensed under a Creative Commons Attribution-NonCommercial 3.0 Unported Licence.

Table 2 The results of liver microsome stability tests expressed in terms intrinsic clearance (CL_{int}) and relative to the positive control diazepam

Compound	4a	4b	4c	4d	4e	4f
CL_{int} (μL min^{-1} mg^{-1} protein)	34	105	83	132	97	239
Cpd CL_{int}/diazepam CL_{int}	1.8	2.0	4.4	6.9	5.1	12.5

binding of the sulfonylphenoxazines into site 2 is primarily responsible for their inhibition of $Ca_V2.2$ ion channels. Qualitatively, docking site 1 is a larger pocket, rich in polar and charged residues, and in contact with water. It appears less suited for binding lipophilic molecules like the sulfonylphenoxazines, compared to docking site 2 and 3, which are located in the transmembrane and are rich with lipophilic residues.

The series in which the ether linkage was replaced with an amine (**10a–10f**, **12** and **14**) was prepared in the hope that additional hydrogen bond and/or salt bridge associations would improve the affinity to the $Ca_V2.2$ channel. In most cases, this change had a limited or even slightly detrimental effect on channel affinities, with only the imidazole **10d** showing a marked improvement. Consistent with this, no interactions with either the aryl ether oxygen of **4a–4f** or the aniline nitrogen of **10a–10f** could be detected in the structures docked into the cryo-EM structure of the channel.

In vitro metabolic stability assessments

Six sulfonylphenoxazines (**4a–4f**) were assessed for their stability in male rat plasma using diazepam as a positive control. In stark contrast to that previously reported for the acylphenoxazine **1b**, which was found to hydrolyse with a $t_{1/2}$ = 13.9 min,[14] only the monomethylamine **4a** showed any significant degradation, with an average of 73 ± 5% remaining after 24 hours. Greater than 90% of the other five sulfonylphenoxazines (**4b–4f**) remained intact after the same period. The same six sulfonylphenoxazines were also subjected to an *in vitro* liver microsome stability test, this time using diazepam as the control. The results are presented in Table 2 both in terms of an intrinsic clearance (CL_{int}), which is equivalent to k_{cat}/K_m for a single enzyme reaction, and a ratio of a compound's CL_{int} to that measured for diazepam. LCMS analysis of the assay mixtures showed that hydroxylation was a major metabolic route for all six compounds, together with demethylation for the methylamines **4a** and **4b**. Given that diazepam is considered to be a long-acting drug in humans, with a $t_{1/2}$ = 20–35 h in the body, the methylamines **4a** and **4b** in particular showed promising stability.

Potential to penetrate the blood–brain barrier

An obvious consideration when attempting to develop central nervous system (CNS)-active drugs is their potential to cross the blood–brain barrier and enter the CNS. A widely used predicter developed by Pfizer scientists is the CNS MPO desirability tool,[15,16] which uses a set of six physico-chemical properties to rank compounds on a scale of 0–6 in terms of their likelihood to penetrate the CNS. A score ≥4 suggests that a compound is likely to be able to enter the CNS. The CNS MPO scores calculated for the sulfonylphenoxazines prepared in this study are shown in Table 3. With the exception of the piperidine derivatives **4e** and **10e**, the sulfonylphenoxazines yielded highly favourable CNS MPO scores (4.0–4.5), with **4b** in particular showing an improved MPO score (4.5) over the previously described open chain sulfonamide **16** (4.3).[17] An MPO score of 4.5 is well within the range of many currently prescribed CNS-active drugs.[16] Importantly, **4b** has a similar CNS MPO score to tramadol (4.6) and is superior to the two TCAs clomipramine (3.1) and nortriptyline (3.3), and the two neuropathic pain medications gabapentin (4.2) and pregabalin (4.2).[16]

Conclusions

As was recently reported for open chain phenoxy-substituted $Ca_V2.2$ blockers,[17] the substitution of an acyl link for a sulfonyl functionality in the phenoxazine series has not only led to significantly improved stability in rat plasma, but has also seen a 4–10-fold enhancement in affinity for the target neuronal calcium ion channel, leading to compounds with equivalent effectiveness to the best reported for this class of compound. For the first time, molecular modelling based on a published $Ca_V2.2$ cryo-EM structure, has provided insight

Table 3 Calculated CNS MPO scores for sulfonylphenoxazines **4a–4f**, **10a–10f**, **12** and **14–16**, together with those reported for gabapentin and pregabalin

Compound	Score
4a	4.3
4b	4.5
4c	4.0
4d	4.2
4e	3.4
4f	4.2
10a	4.1
10b	4.5
10c	4.0
10d	4.4
10e	3.6
10f	4.5
12	4.2
14	4.1
15	4.4
16	4.3
Gabapentin	4.2[a]
Pregabalin	4.2[a]

[a] From ref. 16.

Open Access Article. Published on 12 June 2024. Downloaded on 2/3/2026 11:10:36 AM. This article is licensed under a Creative Commons Attribution-NonCommercial 3.0 Unported Licence.

on how this class of channel blockers inhibit the passage of calcium ions through the channel. These results suggest that the ammonium side chains of these inhibitors associate with the channel's selectivity filter and amino acid residues above the selectivity filter engage with the aromatic head structure. This is a region where tricyclic antidepressants like amitriptyline have been predicted to bind, and in so doing, limit the channel's ability to transition from a closed to an open state. Hydrogen bonding to the sulfonyl functionality also appears to be important here, which would explain why the sulfonyl compounds tend to show stronger inhibition than the corresponding acyl derivatives. It was hoped that the replacement of the ether link for an amine would pick up additional interactions however in most cases improved binding strength was not observed. As indicated, most models show the ammonium side chain strongly associating with the carboxylate residues that make up the selectivity filter and consistent with this, the affinity of the methoxy analogue (**15**) was found to be greatly diminished relative to the corresponding methylamine (**4a**).

Again, for the first time, this class of compound was tested for metabolic stability in an *in vitro* liver microsome assay. Hydroxylation and demethylation were found to be the main metabolic routes, with the rate of degradation of the methylamines **4a** and **4b** comparing favourably with the positive control diazepam, a drug that is considered long acting. Finally, the likelihood of the dimethylamine **4b** to enter the CNS, as judged by its calculated MPO score, appears to be high, yielding a value well within the range of many CNS-active drugs and superior to the neuropathic pain medications gabapentin and pregabalin, and the related open chain analogue **16**.

In summary, the replacement of the acyl link in previously reported phenoxazine-based $Ca_V2.2$ inhibitors has led to compounds with improved metabolic stability and affinity for the channel that is equivalent to the best reported for this class of compound. One of the most active compounds (**4b**) is also more likely to penetrate the blood brain barrier, based on its CNS MPO score. In addition, molecular modelling using a recently reported cryo-EM structure of the channel has been employed to predict where in the channel this class of inhibitor binds and how they exert their inhibitory effect. Based on our previous findings, future optimisation of the lead structure will involve exploring substitution of the aromatic rings. Additionally, future studies will investigate the state-dependency of the most active compounds using electrophysiology assays, and will test the most potent lead compound for blood–brain barrier penetration.

Experimental

Chemistry

General experimental. Commercially available reagents and solvents were used as purchased without further purification unless otherwise stated. Air-sensitive reactions were performed under an atmosphere of nitrogen using a standard Schlenk line and glassware for moisture-sensitive reactions were dried overnight in the oven at 110 °C. Dry column vacuum chromatography was conducted using Divisil LC60A silica gel (20–45 μm), following the protocol by Pedersen and Rosenbohm.[24]

Thin-layer chromatography (TLC) was performed using TLC Silica Gel 60 F254 and visualised under UV lamp or through the use of an appropriate stain such as potassium permanganate or ninhydrin. Melting points were recorded in an ISG melting point apparatus.

Proton nuclear magnetic resonance (^{1}H NMR) and Fluorine nuclear magnetic resonance (^{19}F NMR) spectra were recorded on a Bruker AV400 or AV600 as specified. The resonance shifts were assigned based on the chemical shift (δ – measured in ppm), multiplicity (s – singlet, d – doublet, t – triplet, q – quartet, *etc.*), number of protons, observed coupling constant (J – measured in Hz). Carbon-13 nuclear magnetic resonance (^{13}C NMR) spectra were recorded on Bruker AV400 or AV600 at 100 or 150 MHz respectively. All chemical shifts referenced to either TMS or the residual solvent peak unless otherwise stated.

High-resolution mass spectrometry (APCI, ESI) was conducted on a Thermo Scientific QExactive FT-MS. Positive ion EI mass spectra were performed using a Thermo Scientific DFS mass spectrometer using an ionisation energy of 70 eV. Accurate mass measurements were obtained with a resolution of 5000–10 000 using PFK (perfluorokerosene) as the reference compound.

High Performance Liquid Chromatography (HPLC) methods (Methods 1–5) are detailed in the Supplementary Information.

10-((4-(3-Chloropropoxy)phenyl)sulfonyl)-10*H*-phenoxazine (3). Phenoxazine (366 mg, 2.00 mmol) was dissolved in pyridine (5 mL) and cooled to 0 °C then the sulfonylchloride **2** (see ESI†) (538 mg, 2.00 mmol) was added. The mixture was left stirring for 4 hours then the solvent was evaporated. Ethyl acetate (50 mL) was added and the mixture was extracted with 1 M $NaOH_{(aq)}$ (3 × 50 mL). The combined organic layers were dried with magnesium sulfate, filtered and concentrated. Purification by DCVC using 0–100% ethyl acetate in petroleum ether (5% gradient) afforded the title compound as a greenish solid (738 mg, 1.78 mmol, 89%).

^{1}H NMR ($CDCl_3$, 400 MHz) δ (ppm) = 7.69 (dd, J = 7.8, 1.8 Hz, 2H), 7.26–7.12 (m, 4H), 7.07–6.98 (m, 2H), 6.84 (dd, J = 7.9, 1.6 Hz, 2H), 6.76–6.68 (m, 2H), 4.12 (t, J = 5.9 Hz, 2H), 3.74 (t, J = 6.2 Hz, 2H), 2.25 (p, J = 6.1 Hz, 2H).

^{13}C NMR ($CDCl_3$, 100 MHz) δ(ppm) = 162.70, 151.20, 129.93, 128.32, 128.16, 127.43, 126.45, 123.78, 116.28, 114.10, 64.67, 41.14, 31.98.

General procedure 1: synthesis of phenoxazine analogues (4a–4f). The chloro compound **3** and sodium iodide (3 eq.) were suspended in acetonitrile (1 mL per 0.1 mmol) and the mixture was heated to 95 °C in a microwave reactor (120 W) for 2 hours. The amine (3 eq.) was then added and the mixture was left stirring at room temperature for 2 hours. The solvent was then evaporated, and the product was purified by preparative HPLC following Method 1.

 This journal is © The Royal Society of Chemistry 2024

Open Access Article. Published on 12 June 2024. Downloaded on 2/3/2026 11:10:36 AM. This article is licensed under a Creative Commons Attribution-NonCommercial 3.0 Unported Licence.

General procedure 2: general characterisation and determination of TFA equivalents by ^{19}F NMR. The final product was redissolved in MQ water and freeze-dried before purity analysis by analytical HPLC following Method 4, characterisation by HRMS analysis and NMR spectroscopy in methanol-d_4 or acetonitrile-d_3. Fluoroacetonitrile (approx. 5 μL, 0.09 mmol) was then added to the NMR sample of the compound of interest, and proton nuclear magnetic resonance (^{1}H NMR) and Fluorine nuclear magnetic resonance (^{19}F NMR) spectra of the mixture were recorded. The molar ratio of fluoroacetonitrile to the compound of interest was obtained from the ^{1}H NMR spectrum; the ratio of TFA to fluoroacetonitrile is obtained from the ^{19}F NMR spectrum. The ratio of TFA to the compound of interest was then deduced, rounded to the nearest integer to account for experimental uncertainty. The compound of interest was then recovered by concentrating the NMR sample, redissolving it in MQ water and freeze-drying.

3-(4-((10*H*-Phenoxazin-10-yl)sulfonyl)phenoxy)-*N*-methylpropan-1-amine.TFA (4a). The title compound was synthesised from **3** (36 mg, 0.087 mmol) following General Procedure 1, using 40 wt% aq. methylamine, and characterised following General Procedure 2. The product was afforded as a mono-TFA salt (18.38 mg, 40%).

^{1}H NMR (MeOD, 600 MHz) δ (ppm) = 7.62 (dd, J = 8.0, 1.6 Hz, 2H), 7.28 (td, J = 7.8, 1.6 Hz, 2H), 7.21 (td, J = 7.7, 1.4 Hz, 2H), 7.01–6.95 (m, 2H), 6.86 (td, J = 8.0, 1.8 Hz, 4H), 4.13 (t, J = 5.7 Hz, 2H), 3.21 (t, J = 7.3 Hz, 2H), 2.75 (s, 3H), 2.22–2.14 (m, 2H).

^{13}C NMR (MeOD, 150 MHz) δ (ppm) = 162.75, 151.19, 129.68, 128.39, 127.72, 127.41, 126.33, 123.52, 116.01, 114.00, 65.24, 46.67, 32.45, 25.53.

HRMS (APCI): m/z calculated for $[M + H]^+$: 411.1373, found 411.1374.

3-(4-((10*H*-Phenoxazin-10-yl)sulfonyl)phenoxy)-*N*,*N*-dimethylpropan-1-amine.TFA (4b). The compound was synthesised from **3** (45 mg, 0.11 mmol) following General Procedure 1, using 40 wt% aq. dimethylamine, and characterised following General Procedure 2. The product was afforded as a mono-TFA salt (25.05 mg, 44%).

^{1}H NMR (MeOD, 600 MHz) δ (ppm) = 7.62 (dd, J = 8.0, 1.6 Hz, 2H), 7.28 (td, J = 7.8, 1.6 Hz, 2H), 7.21 (td, J = 7.7, 1.4 Hz, 2H), 7.01–6.95 (m, 2H), 6.89–6.83 (m, 4H), 4.13 (t, J = 5.8 Hz, 2H), 3.36–3.33 (m, 2H), 2.95 (s, 6H), 2.27–2.19 (m, 2H).

^{13}C NMR (MeOD, 150 MHz) δ (ppm) = 162.73, 151.20, 129.69, 128.39, 127.73, 127.41, 126.33, 123.52, 116.02, 113.99, 65.00, 55.10, 42.20, 24.08.

HRMS (APCI): m/z calculated for $[M + H]^+$: 425.1530, found 425.1526.

10-((4-(3-(Pyrrolidin-1-yl)propoxy)phenyl)sulfonyl)-10*H*-phenoxazine.TFA (4c). The compound was synthesised from **3** (36 mg, 0.087 mmol) following General Procedure 1 and characterised following General Procedure 2. The product was afforded as a mono-TFA salt (43.59 mg, 89%).

^{1}H NMR (MeOD, 600 MHz) δ (ppm) = 7.61 (dd, J = 8.0, 1.6 Hz, 2H), 7.28 (td, J = 7.8, 1.7 Hz, 2H), 7.20 (td, J = 7.7, 1.4 Hz, 2H), 7.00–6.95 (m, 2H), 6.87–6.81 (m, 4H), 4.11 (t, J = 5.8 Hz, 2H), 3.63–3.56 (m, 2H), 3.32–3.26 (m, 2H), 2.97 (td, J = 12.6, 3.0 Hz, 2H), 2.28–2.20 (m, 2H), 2.02–1.95 (m, 2H), 1.91–1.73 (m, 3H), 1.60–1.49 (m, 1H).

^{13}C NMR (MeOD, 150 MHz) δ (ppm) = 162.76, 151.19, 129.70, 128.41, 127.71, 127.34, 126.31, 123.52, 116.03, 113.96, 65.06, 54.18, 53.05, 23.58, 22.90, 21.27.

HRMS (APCI): m/z calculated for $[M + H]^+$: 451.1686, found 451.1685.

10-((4-(3-(1*H*-Imidazol-1-yl)propoxy)phenyl)sulfonyl)-10*H*-phenoxazine.TFA (4d). The compound was synthesised from **3** (13 mg, 0.031 mmol) following General Procedure 1 and characterised following General Procedure 2. The product was afforded as a mono-TFA salt (6.49 mg, 37%).

^{1}H NMR (MeOD, 600 MHz) δ (ppm) = 8.99 (s, 1H), 7.69 (t, J = 1.8 Hz, 1H), 7.62 (dd, J = 8.0, 1.6 Hz, 2H), 7.59 (t, J = 1.7 Hz, 1H), 7.28 (td, J = 7.7, 1.8 Hz, 2H), 7.21 (td, J = 7.5, 1.3 Hz, 2H), 7.00–6.94 (m, 2H), 6.86 (dd, J = 8.1, 1.4 Hz, 2H), 6.83–6.77 (m, 2H), 4.48 (t, J = 7.0 Hz, 2H), 4.10 (t, J = 5.7 Hz, 2H), 2.40 (p, J = 6.2 Hz, 2H).

^{13}C NMR (MeOD, 150 MHz) δ (ppm) = 162.70, 151.21, 135.23, 129.70, 128.39, 127.73, 127.37, 126.34, 123.52, 122.05, 119.84, 116.01, 113.90, 64.93, 46.53, 29.11.

HRMS (APCI): m/z calculated for $[M + H]^+$: 448.1326, found 448.1327.

10-((4-(3-(Piperidin-1-yl)propoxy)phenyl)sulfonyl)-10*H*-phenoxazine.TFA (4e). The compound was synthesised from **3** (36 mg, 0.087 mmol) following General Procedure 1 and characterised following General Procedure 2. The product was afforded as a mono-TFA salt (34.49 mg, 0.059 mmol, 68%).

^{1}H NMR (MeOD, 600 MHz) δ (ppm) = 7.61 (dd, J = 8.0, 1.6 Hz, 2H), 7.28 (td, J = 7.8, 1.6 Hz, 2H), 7.20 (td, J = 7.7, 1.4 Hz, 2H), 7.00–6.95 (m, 2H), 6.88–6.81 (m, 4H), 4.12 (t, J = 5.8 Hz, 2H), 3.83–3.55 (m, 2H), 3.43–3.37 (m, 2H), 3.13 (s, 2H), 2.30–1.98 (m, 6H).

^{13}C NMR (MeOD, 150 MHz) δ (ppm) = 162.76, 151.20, 129.70, 128.40, 127.72, 127.36, 126.32, 123.52, 116.02, 113.98, 64.98, 53.96, 52.17, 48.19, 25.43, 22.57.

HRMS (APCI): m/z calculated for $[M + H]^+$: 465.1843, found 465.1845.

10-((4-(3-Morpholinopropoxy)phenyl)sulfonyl)-10*H*-phenoxazine.TFA (4f). The compound was synthesised from **3** (17 mg, 0.041 mmol) following General Procedure 1 and characterised following General Procedure 2. The product was afforded as a mono-TFA salt (11.87 mg, 50%).

^{1}H NMR (MeOD, 600 MHz) δ (ppm) = 7.62 (dd, J = 8.0, 1.6 Hz, 2H), 7.28 (td, J = 7.9, 1.6 Hz, 2H), 7.21 (td, J = 7.7, 1.4 Hz, 2H), 7.02–6.94 (m, 2H), 6.89–6.83 (m, 4H), 4.17–4.04 (m, 4H), 3.83–3.74 (m, 2H), 3.60–3.52 (m, 2H), 3.41–3.32 (m, 2H), 3.25–3.15 (m, 2H), 2.30–2.22 (m, 2H).

^{13}C NMR (MeOD, 150 MHz) δ (ppm) = 162.71, 151.20, 129.72, 128.39, 127.73, 127.47, 126.34, 123.53, 116.00, 113.96, 64.93, 63.69, 54.46, 51.92, 23.27.

HRMS (APCI): m/z calculated for $[M + H]^+$: 467.1635, found 467.1636.

Open Access Article. Published on 12 June 2024. Downloaded on 2/3/2026 11:10:36 AM. This article is licensed under a Creative Commons Attribution-NonCommercial 3.0 Unported Licence.

10-((4-Nitrophenyl)sulfonyl)-10*H*-phenoxazine (6). Phenoxazine (366 mg, 2.00 mmol) was dissolved in pyridine (4 mL) and cooled to 0 °C then 4-nitrobenzene sulfonyl chloride (**5**) (442 mg, 2.00 mmol) was added. The mixture was left stirring overnight then the solvent was evaporated. 0.25 M $NaOH_{(aq)}$ (25 mL) was added and the product was extracted with chloroform (3 × 25 mL). The combined organic layers were dried with magnesium sulfate, filtered and concentrated, affording the compound as a red solid (680 mg, 92%).

MP: 170–172 °C.

^{1}H NMR ($CDCl_3$, 400 MHz) δ (ppm) = 8.15–8.07 (m, 2H), 7.70 (dd, J = 7.8, 1.8 Hz, 2H), 7.33–7.18 (m, 6H), 6.86 (dd, J = 7.9, 1.6 Hz, 2H).

^{13}C NMR ($CDCl_3$, 100 MHz) δ (ppm) = 151.09, 141.00 (HMBC), 129.02, 128.98, 127.96, 125.67, 124.24, 123.56, 116.65.

4-((10*H*-Phenoxazin-10-yl)sulfonyl)aniline (7). The nitro compound **6** (150 mg, 0.51 mmol) and palladium on carbon (15 mg, 10 wt%) added to ethanol (10 mL), then the mixture was deoxygenated for 15 minutes under a stream of nitrogen. Hydrazine hydrate 50% solution in water (630 μL, 10.0 mmol) was then added, and the mixture was left stirring at reflux overnight. The mixture was then filtered through a pad of silica, then the solvent was evaporated. The product was redissolved in ethyl acetate (20 mL) and washed with distilled water (3 × 20 mL). The organic layer was dried over anhydrous magnesium sulfate, filtered and concentrated to give the title compound as a red solid (153 mg, 88%).

MP: 110–112 °C.

^{1}H NMR ($CDCl_3$, 400 MHz) δ (ppm) = 7.67 (dd, J = 7.8, 1.8 Hz, 2H), 7.24–7.12 (m, 5H), 6.90–6.79 (m, 4H), 6.49 (d, J = 8.5 Hz, 2H).

^{13}C NMR ($CDCl_3$, 100 MHz) δ 151.24, 150.93, 129.87, 128.22, 128.14, 126.65, 123.95, 123.66, 116.19, 113.58.

***N*-(4-((10*H*-Phenoxazin-10-yl)sulfonyl)phenyl)-3-chloropropanamide (8).** The aniline **7** (272 mg, 0.80 mmol) was dissolved in DCM (9 mL) and pyridine (1 mL) then chloropropionyl chloride (95 μL, 1 mmol) was added and the mixture was left stirring for 1.5 h. 0.25 M $NaOH_{(aq)}$ (25 mL) was then added and the product was extracted with chloroform (3 × 25 mL). The combined organic layers were dried with magnesium sulfate, filtered through silica and concentrated, affording the compound as an orange oil (339 mg, 99%).

^{1}H NMR ($CDCl_3$, 400 MHz) δ (ppm) = 7.58 (dd, J = 7.8, 1.8 Hz, 2H), 7.41–7.35 (m, 2H), 7.16–7.05 (m, 5H), 6.98–6.91 (m, 2H), 6.74 (dd, J = 7.9, 1.6 Hz, 2H), 3.78 (t, J = 6.3 Hz, 2H), 2.76 (t, J = 6.3 Hz, 2H).

^{13}C NMR ($CDCl_3$, 100 MHz) δ (ppm) = 168.01, 151.17, 142.28, 130.48, 129.11, 128.50, 128.05, 126.22, 123.87, 118.64, 116.43, 40.52, 39.41.

4-((10*H*-Phenoxazin-10-yl)sulfonyl)-*N*-(3-chloropropyl) aniline (9). Adapted from a procedure of Fukuda *et al.*,[25] the amide **8** (339 mg, 0.79 mmol) was dissolved in 4 mL dry THF under nitrogen then 8 mL of a 1 M BH_3 solution in THF (8 mmol) was added and the mixture was left stirring at reflux for 2 h. The solvent was evaporated and $NaHCO_{3(aq)}$ (25 mL) was added, and the product was extracted with chloroform (3 × 25 mL). The combined organic layers were dried over anhydrous magnesium sulfate, filtered and concentrated. Purification by DCVC using 0 to 100% ethyl acetate in petroleum ether (4% gradient) afforded the compound as a dark yellow oil (195 mg, 0.47 mmol, 66%).

^{1}H NMR ($CDCl_3$, 400 MHz) δ (ppm) = 8.55 (s, 1H), 7.58 (dd, J = 7.9, 1.8 Hz, 2H), 7.15–7.00 (m, 4H), 6.80–6.68 (m, 4H), 6.30–6.16 (m, 2H), 3.55 (t, J = 6.4 Hz, 2H), 3.25 (t, J = 6.7 Hz, 2H), 2.02–1.87 (m, 2H).

^{13}C NMR ($CDCl_3$, 100 MHz) δ (ppm) = 151.88, 151.25, 147.56, 139.00, 129.86, 128.24, 128.11, 126.72, 125.30, 123.64, 122.49, 116.16, 111.14, 42.25, 40.38, 31.54.

General procedure 3 – synthesis of phenoxazine–aniline analogues (10a–10f). The chloro compound **9** and sodium iodide (10 eq.) were suspended in THF (2 mL), then the amine (10 eq.) was added and the mixture was heated to 95 °C in a microwave reactor (120 W) for 1 hour. The mixture was filtered and purified by preparative HPLC following Method 1.

***N*^{1}-(4-((10*H*-Phenoxazin-10-yl)sulfonyl)phenyl)-*N*^{3}-methylpropane-1,3-diamine.2TFA (10a).** The compound was synthesised from **9** (20 mg, 0.050 mmol) following General Procedure 3, using 40 wt% aq. methylamine, and characterised following General Procedure 2. The product was afforded as a di-TFA salt (3.85 mg, 12%).

^{1}H NMR (MeOD, 400 MHz) δ (ppm) = 7.49 (dd, J = 7.9, 1.6 Hz, 2H), 7.17 (td, J = 7.8, 1.6 Hz, 2H), 7.08 (td, J = 7.7, 1.5 Hz, 2H), 6.77 (dd, J = 8.1, 1.4 Hz, 2H), 6.70–6.61 (m, 2H), 6.37–6.29 (m, 2H), 3.13 (td, J = 8.2, 7.5, 4.2 Hz, 4H), 2.62 (s, 3H), 1.97–1.85 (m, 2H).

^{13}C NMR (MeOD, 100 MHz) δ (ppm) = 152.94 (HMBC), 151.29, 129.48, 128.14, 127.78, 126.62, 123.30, 120.93, 115.93, 110.51, 55.55, 42.13, 39.26, 23.69.

HRMS (APCI): m/z calculated for $[M + H]^+$: 410.1533, found 410.1533.

***N*^{1}-(4-((10*H*-Phenoxazin-10-yl)sulfonyl)phenyl)-*N*^{3},*N*^{3}-dimethylpropane-1,3-diamine.2TFA (10b).** The compound was synthesised from **9** (22 mg, 0.053 mmol) following General Procedure 3, using 40 wt% aq. dimethylamine, and characterised following General Procedure 2. The product was afforded as a di-TFA salt (15.87 mg, 46%).

^{1}H NMR (MeOD, 400 MHz) δ 7.59 (dd, J = 7.9, 1.6 Hz, 2H), 7.22 (dtd, J = 32.4, 7.6, 1.6 Hz, 4H), 6.89–6.72 (m, 4H), 6.49–6.34 (m, 2H), 3.26–3.17 (m, 4H), 2.90 (s, 6H), 2.06–1.93 (m, 2H).

^{13}C NMR (MeOD, 100 MHz) δ 152.97 (HMBC), 151.28, 129.49, 128.11, 127.80, 126.64, 123.30, 121.03, 115.90, 110.48, 55.56, 42.12, 39.24, 23.71.

HRMS (APCI): m/z calculated for $[M + H]^+$: 424.1689, found 424.1690.

4-((10*H*-Phenoxazin-10-yl)sulfonyl)-*N*-(3-(pyrrolidin-1-yl) propyl)aniline.2TFA (10c). The compound was synthesised from **9** (30 mg, 0.073 mmol) following General Procedure 3

 This journal is © The Royal Society of Chemistry 2024

Open Access Article. Published on 12 June 2024. Downloaded on 2/3/2026 11:10:36 AM. This article is licensed under a Creative Commons Attribution-NonCommercial 3.0 Unported Licence.

and characterised following General Procedure 2. The product was afforded as a di-TFA salt (21.28 mg, 43%).

^{1}H NMR (MeOD, 400 MHz) δ (ppm) = 7.59 (dd, J = 7.9, 1.7 Hz, 2H), 7.31–7.13 (m, 4H), 6.86 (dd, J = 8.1, 1.5 Hz, 2H), 6.78–6.71 (m, 2H), 6.46–6.37 (m, 2H), 3.71–3.62 (m, 2H), 3.30–3.20 (m, 6H), 3.14–3.03 (m, 2H), 2.23–1.95 (m, 6H).

^{13}C NMR (MeOD, 100 MHz) δ (ppm) = 152.92 (HMBC), 151.29, 129.49, 128.10, 127.79, 126.66, 123.29, 121.00 (HMBC), 115.90, 110.48, 53.91, 52.73, 39.33, 25.12, 22.57.

HRMS (APCI): m/z calculated for $[M + H]^+$: 450.1846, found 450.1843.

4-((10*H*-Phenoxazin-10-yl)sulfonyl)-*N*-(3-(1*H*-imidazol-1-yl) propyl)aniline.2TFA (10d). The compound was synthesised from **9** (30 mg, 0.073 mmol) following General Procedure 3 and characterised following General Procedure 2. The product was afforded as a di-TFA salt (5.44 mg, 11%).

^{1}H NMR (MeOD, 600 MHz) δ (ppm) = 8.77 (s, 1H), 7.62–7.57 (m, 3H), 7.51 (s, 1H), 7.26 (td, J = 7.7, 1.7 Hz, 2H), 7.18 (td, J = 7.7, 1.5 Hz, 2H), 6.86 (dd, J = 8.1, 1.4 Hz, 2H), 6.78–6.72 (m, 2H), 6.41–6.35 (m, 2H), 4.34 (t, J = 7.2 Hz, 2H), 3.17 (t, J = 6.7 Hz, 2H), 2.18 (p, J = 6.9 Hz, 2H).

^{13}C NMR (MeOD, 100 MHz) δ 153.00, 151.29, 135.07, 129.46, 128.14, 127.78, 126.62, 123.30, 121.87, 120.22, 115.93, 110.46, 104.98, 46.88, 39.06, 28.87.

HRMS (APCI): m/z calculated for $[M + H]^+$: 447.1485, found 447.1485.

4-((10*H*-Phenoxazin-10-yl)sulfonyl)-*N*-(3-(piperidin-1-yl) propyl)aniline.2TFA (10e). The compound was synthesised from **9** (30 mg, 0.073 mmol) following General Procedure 3 and characterised following General Procedure 2. The product was afforded as a di-TFA salt (9.95 mg, 20%).

^{1}H NMR (CD_3CN, 600 MHz) δ 7.47 (dd, J = 8.0, 1.6 Hz, 2H), 7.17 (td, J = 7.8, 1.6 Hz, 2H), 7.08 (td, J = 7.7, 1.4 Hz, 2H), 6.77 (dd, J = 8.1, 1.4 Hz, 2H), 6.62 (d, J = 8.9 Hz, 2H), 6.31–6.24 (m, 2H), 3.33 (d, J = 12.2 Hz, 2H), 3.02 (t, J = 6.6 Hz, 2H), 2.98–2.90 (m, 2H), 2.66 (d, J = 14.1 Hz, 2H), 1.87 (dd, J = 9.9, 4.9 Hz, 2H), 1.79–1.58 (m, 6H).

^{13}C NMR (CD_3CN, 150 MHz) δ 153.66, 151.87, 130.35, 129.28, 128.66, 127.32, 124.46, 121.63, 116.97, 111.55, 55.22, 53.70, 40.40, 23.61, 23.37, 22.07.

HRMS (ESI): m/z calculated for $[M + H]^+$: 464.2002, found: 464.2004.

4-((10*H*-Phenoxazin-10-yl)sulfonyl)-*N*-(3-morpholinopropyl) aniline.2TFA (10f). The compound was synthesised from **9** (30 mg, 0.073 mmol) following General Procedure 3 and characterised following General Procedure 2. The product was afforded as a di-TFA salt (19.47 mg, 39%).

^{1}H NMR (MeOD, 600 MHz) δ (ppm) = 7.59 (dd, J = 8.0, 1.6 Hz, 2H), 7.25 (td, J = 7.7, 1.6 Hz, 2H), 7.18 (td, J = 7.7, 1.4 Hz, 2H), 6.86 (dd, J = 8.1, 1.4 Hz, 2H), 6.79–6.73 (m, 2H), 6.45–6.39 (m, 2H), 4.12–4.02 (m, 2H), 3.81–3.71 (m, 2H), 3.50 (d, J = 12.5 Hz, 2H), 3.28–3.21 (m, 4H), 3.19–3.09 (m, 2H), 2.07–1.98 (m, 2H).

^{13}C NMR (MeOD, 150 MHz) δ (ppm) = 152.89, 151.28, 129.49, 128.10, 127.78, 126.64, 123.28, 121.06, 115.91, 110.48, 63.64, 55.01, 51.86, 39.30, 22.89.

HRMS (APCI): m/z calculated for $[M + H]^+$: 466.1795, found 466.1794.

4-((10*H*-Phenoxazin-10-yl)sulfonyl)-*N*-(3-chloropropyl)-*N*-methylaniline (11). The chloro compound **9** (26 mg, 0.063 mmol) was dissolved in ACN (3 mL), then TFA (0.3 mL), paraformaldehyde (100 mg, 3.3 mmol, 50 eq.) and sodium cyanoborohydride (200 mg, 3.3 mmol, 50 eq.) were added and the mixture was left stirring at reflux overnight. 0.25 M $NaOH_{(aq)}$ (25 mL) was added and the product was extracted with chloroform (3 × 25 mL). The combined organic layers were dried with magnesium sulfate, filtered over silica and concentrated. Purification by DCVC using 0 to 100% ethyl acetate in petroleum ether (5% gradient) was attempted, but the title compound **11** was obtained as an approximately 4 to 1 mixture with the starting material **9**, as a thick yellow oil (24 mg, ~89%), and was used for the next step without further purification.

***N*^{1}-(4-((10*H*-Phenoxazin-10-yl)sulfonyl)phenyl)-*N*^{1},*N*^{3},*N*^{3}-trimethylpropane-1,3-diamine.2TFA (12).** The chloro compound **11** (approximately 0.047 mmol) and sodium iodide (75 mg, 0.5 mmol, 10 eq.) were suspended in THF (1 mL), then dimethylamine (0.5 mL of a 2 M solution in THF, 1 mmol) was added and the mixture was heated to 95 °C in a microwave reactor (120 W) for 1 hour. The mixture was filtered and purified by preparative HPLC following Method 1 then Method 3, and characterised following General Procedure 2. The title compound was afforded as a di-TFA salt (5.07 mg, 16%).

^{1}H NMR (CD_3CN, 600 MHz) δ 7.53 (dd, J = 8.0, 1.6 Hz, 2H), 7.21 (td, J = 7.7, 1.6 Hz, 2H), 7.13 (td, J = 7.7, 1.4 Hz, 2H), 6.81 (dd, J = 8.1, 1.4 Hz, 2H), 6.74–6.69 (m, 2H), 6.47–6.41 (m, 2H), 3.34 (t, J = 7.4 Hz, 2H), 2.97–2.89 (m, 2H), 2.86 (s, 3H), 2.67 (s, 6H), 1.88–1.83 (m, 2H + CD_3CN).

^{13}C NMR (CD_3CN, 150 MHz,) δ 153.27, 151.86, 130.16, 129.25, 128.65, 127.34, 124.43, 121.18, 116.98, 111.16, 55.40, 49.31, 43.06, 38.24, 22.28.

HRMS (ESI): m/z calculated for $[M + H]^+$: 438.1846, found: 438.1849.

***N*-(4-((10*H*-Phenoxazin-10-yl)sulfonyl)phenyl)piperidin-4-amine.2TFA (14).** The aniline **7** (58 mg, 0.172 mmol) was dissolved in DCE (2 mL) then acetic acid (20 μL, 0.343 mmol), *N*-boc-4-piperidine (68 mg, 0.344 mmol) and sodium triacetoxyborohydride (110 mg, 0.516 mmol) were added. The mixture was left stirring at reflux over the weekend then one additional equivalent of acetic acid (20 μL, 0.343 mmol), *N*-boc-4-piperidine (68 mg, 0.344 mmol) and sodium triacetoxyborohydride (110 mg, 0.516 mmol) were added. 1 M $NaOH_{(aq)}$ (25 mL) was then added and the product was extracted with chloroform (3 × 25 mL) and the extracts concentrated. The Boc-protected product was then redissolved in DCM (3 mL), and triisopropyl silane (50 μL), water (50 μL) and TFA (1 mL) were added. The mixture was left stirring overnight, then the solvent was evaporated. The amine product was then purified by preparative HPLC following Method 2 and characterised following General Procedure 2. The title compound was afforded as a di-TFA salt (4.60 mg, 6%).

Open Access Article. Published on 12 June 2024. Downloaded on 2/3/2026 11:10:36 AM. This article is licensed under a Creative Commons Attribution-NonCommercial 3.0 Unported Licence.

^{1}H NMR (MeOD, 600 MHz) δ (ppm) = 7.59 (dd, J = 8.0, 1.6 Hz, 2H), 7.25 (td, J = 7.9, 1.4 Hz, 2H), 7.18 (td, J = 7.6, 1.4 Hz, 2H), 6.86 (dd, J = 8.1, 1.4 Hz, 2H), 6.79–6.73 (m, 2H), 6.49–6.43 (m, 2H), 3.67–3.61 (m, 1H), 3.48–3.41 (m, 2H), 3.14 (td, J = 12.6, 3.1 Hz, 2H), 2.20 (dd, J = 14.6, 3.8 Hz, 2H), 1.67 (dtd, J = 14.2, 10.6, 3.9 Hz, 2H).

^{13}C NMR (MeOD, 150 MHz) δ (ppm) = 151.76, 151.31, 129.54, 128.09, 127.80, 126.66, 123.28, 121.11, 115.90, 110.81, 46.20, 42.67, 28.30.

HRMS (APCI): m/z calculated for $[M + H]^+$: 421.1455, found 421.1456.

10-((4-(3-Methoxypropoxy)phenyl)sulfonyl)-10*H*-phenoxazine (15). The chloro compound **3** (41 mg, 0.10 mmol) and sodium iodide (45 mg, 0.3 mmol, 3 eq.) were suspended in THF (1.5 mL) and the mixture was heated to 95 °C in a microwave reactor (120 W) for 3 hours. Methanol (1 mL) and sodium methoxide (10 mg, 0.2 mmol, 2 eq.) were then added and the mixture was heated to 100 °C in a microwave reactor (120 W) for 1 h 30. An additional portion of sodium methoxide (54 mg, 1 mmol, 10 eq.) was added and the mixture was heated to 100 °C in a microwave reactor (120 W) for a further 1 h. Purification by DCVC using 0 to 100% ethyl acetate in petroleum ether (5% gradient), followed by preparative HPLC following Method 3, afforded the title compound as a white solid (10.33 mg, 25%). No trace of TFA was detected on NMR spectroscopy.

^{1}H NMR (600 MHz, Methanol-d_4) δ 7.61 (dd, J = 7.9, 1.6 Hz, 2H), 7.31–7.25 (m, 2H), 7.20 (td, J = 7.7, 1.4 Hz, 2H), 6.97–6.92 (m, 2H), 6.88 (dd, J = 8.1, 1.4 Hz, 2H), 6.84–6.79 (m, 2H), 4.60 (s, 3H), 4.08 (t, J = 6.3 Hz, 2H), 3.56 (t, J = 6.2 Hz, 2H), 2.03 (p, J = 6.2 Hz, 2H).

^{13}C NMR (150 MHz, MeOD) δ 163.44, 151.25, 129.64, 128.37, 127.70, 126.63, 126.36, 123.43, 116.05, 113.91, 68.54, 65.04, 57.48, 28.90.

HRMS (ESI): m/z calculated for $[M + H]^+$: 412.1213, found: 412.1211.

Biological evaluations

Calcium influx assays. Calcium flux imaging assays with human neuroblastoma SH-SY5Y cells were performed in the presence of the Ca_V1 blocker nifedipine, to measure the ability of the test compounds to inhibit $Ca_V2.2$ ion channels, cilnidipine was used as a positive control, as previously described.[5,14,17] A similar calcium flux imaging assay was used to measure the ability of the test compounds to inhibit $Ca_V3.2$ channels recombinantly expressed in HEK293T cells.[14,17] The HEK293T were obtained from American Type Culture Collection (ATCC) and the SH-SY5Y human neuroblastoma cells were a kind gift from Victor Diaz (Max Planck Institute for Experimental Medicine, Goettingen, Germany). Briefly, neuroblastoma SH-SY5Y and HEK293T cells were seeded at 40 000 and 10 000 cells per well, respectively, in 384 well flat clear-bottom black plates (Corning, NY, USA) and cultured at 37 °C in a humidified 5% CO_2 incubator 48 h before assay. Cells were loaded with 20 μL per well of Calcium 6 dye (Molecular Devices) reconstituted in assay buffer containing (in mM) 140 NaCl, 11.5 glucose, 5.9 KCl, 1.4 $MgCl_2$, 1.2 NaH_2PO_4, 5 $NaHCO_3$, 1.8 $CaCl_2$,10 HEPES pH 7.4 and 0.1% bovine serum albumin (BSA, Sigma), and incubated for 30 min at 37 °C in a humidified 5% CO_2 incubator. Nifedipine 10 μM (Ca_V1 blocker) was added to the dye solution for $Ca_V2.2$ assay. The Ca^{2+} fluorescence responses were recorded at excitation 470–495 nm and emission 515–575 nm for 10 s to set the baseline, 300 s after addition of compound and for further 300 s after channel activation induced by the addition of 90 mM KCl and 5 mM $CaCl_2$ for $Ca_V2.2$, or 40 mM KCl and 5 mM $CaCl_2$ for $Ca_V3.2$. Compound stock solutions were prepared at 100 mM in 100% DMSO and diluted further in the assay buffer to 1% DMSO, for the highest tested concentration of 100 μM of compound, and serial-diluted 3-fold in assay buffer.

Rat plasma stability assessments

Six sulfonylphenoxazines (**4a–4f**) were assessed for their stability in male rat plasma using diazepam as a positive control, using a protocol adapted from that previously reported.[14] Male rat plasma sourced from Sprague Dawley was purchased from Monash Animal Research Platform (MARP) and stored at −80 °C. Samples were defrosted at room temperature prior to usage. Male rat blood plasma (597 μL) was incubated at 37 °C for thirty minutes, then 3 μL of a 30 mM solution of the compound of interest (final concentration: 150 μM) and diazepam (internal standard, final concentration: 150 μM) in DMSO were added. The mixture was left incubating at 37 °C for 24 h; aliquots of 40 μL were removed at t = 0, 5, 15, 30, 45, 60, 75, 90, 105, 120, 180 and 3600 min, and immediately quenched by adding 40 μL of ACN. The samples were vortexed, diluted with 120 μL of deionized water, vortexed again, cooled on ice for 30 min and finally centrifuged at 10 000 rcf for 15 min. The supernatant solution was then collected and stored at 4 °C until analysis by HPLC following Method 4.

For each compound of interest, the experiment was repeated in triplicate alongside one positive control experiment with diltiazem. The amount of compound of interest remaining at the various time points was determined from the peak area ratio of compound to diazepam. The data was then plotted and, where appropriate, fitted to a one-phase decay model using GraphPad Prism 8.0.2. Representative chromatograms are included in ESI.†

Liver microsome stability assessments

Phosphate-buffered saline (277 μL, pH = 7.4) was incubated at 37 °C for twenty minutes, then 32 μL of a freshly prepared 10 mM NADPH solution (final concentration: 1 mM), 3.2 μL of a 100 μM stock solution of the compound of interest (ACN 1 : 1 water, final concentration 1 μM) and 8 μL of a solution of a 20 mg mL^{-1} male rat liver microsomes (Sigma-Aldrich: reference number M9066; stored at −80 °C until used; final concentration 0.5 mg mL^{-1}) were added. The mixture was left

 This journal is © The Royal Society of Chemistry 2024

Open Access Article. Published on 12 June 2024. Downloaded on 2/3/2026 11:10:36 AM. This article is licensed under a Creative Commons Attribution-NonCommercial 3.0 Unported Licence.

incubating at 37 °C for one hour; aliquots of 30 μL were removed at t = 0, 5, 10, 15, 20, 25, 30, 40, and 60 min, and immediately quenched by adding 60 μL of a solution of 0.5% TFA in methanol. The samples were vortexed, cooled on ice for 30 min and finally centrifugated at 10 000 rcf for 15 min. The supernatant solution was then collected and analysed by LC/HRMS following Method 5.

For each compound of interest, the experiment was repeated in triplicate alongside one positive control experiment with diazepam. For each sample, the chromatogram of the ion corresponding to the compound of interested was extracted. A calibration curve was made in order to determine the amount of compound of interest remaining at each time point. The data was then plotted and fitted to a one-phase decay model using GraphPad Prism 8.0.2. Representative chromatograms are attached in ESI.†

Computational methods

The cryo-EM structure of the α1 subunit of the N-type calcium channel determined by Gao *et al.* (PDB: 7MIY)[18] was imported into Schrödinger Maestro® (version 2021-3).[20] The Small-Molecule Drug Discovery Suite was used to perform docking studies. Using the receptor grid generation utility, docking grids for the three sites of interest were generated by defining a 20 × 20 × 20 Å^3 box around the centroid of the following segments (approximately represented on Fig. 3):

- Docking site 1: $P2_{III}$ and $P2_{IV}$ segments.
- Docking site 2: $S5_{III}$, $S6_{III}$ and $S6_{IV}$ segments.
- Docking site 3: lower parts of the $S6_{I}$, $S6_{II}$, $S6_{III}$ and $S6_{IV}$ segments.

The structures of the compounds of interest were then imported and their possible ionization states at pH = 7.4 ± 2.0 were generated using the LigPrep utility. Rigid docking of the compounds of interest was performed with the docking grid corresponding to sites 1, 2 and 3 using the Glide Ligand Docking utility. Docking scores were exported and plotted in GraphPad 8.0.2 for analysis. Fig. 3 and 5 were generated using the Visual Molecular Dynamics (VMD) 1.9.3 package. VMD was developed by the Theoretical and Computational Biophysics Group in the Beckman Institute for Advanced Science and Technology at the University of Illinois at Urbana-Champaign.[26]

Author contributions

Synthesis: MS. Calcium influx bioassays: MH, YD, FCC. Rat plasma stability and liver microsomal stability: MS. Data analysis: MS, FCC, MH, YD, RJL. Computational methods: MS, MK. Manuscript preparation: PJD, KLT. Project conception and supervision: PJD, KLT.

Conflicts of interest

There are no conflicts to declare.

Acknowledgements

Monash University and CSIRO are acknowledged for funding. This work was also supported by a NHMRC Program Grant (APP1072113, RJL) and NHMRC Fellowship (1119056, RJL). We gratefully acknowledge Dr David Chalmers (MIPS, Monash University, Australia) for providing access to Schrödinger software.

Notes and references

1 D. Bouhassira, M. Lantéri-Minet, N. Attal, B. Laurent and C. Touboul, *Pain*, 2008, **136**, 380.
2 A. S. Fisher, M. T. Lanigan, N. Upton and L. A. Lione, *Front. Pharmacol.*, 2021, **11**, 614990.
3 S. Y. Yoon and J. Oh, *Korean J. Intern. Med.*, 2018, **33**, 1058.
4 S. Sindrup, M. Otto, N. B. Finnerup and T. S. Jensen, *Basic Clin. Pharmacol. Toxicol.*, 2005, **96**, 399.
5 F. C. Cardoso, M. Schmit, M. J. Kuiper, R. J. Lewis, K. L. Tuck and P. J. Duggan, *RSC Med. Chem.*, 2022, **13**, 183.
6 K. E. Galluzzi, *J. Am. Osteopath. Assoc.*, 2005, **105**, S12.
7 G. Cruccu and A. Truini, *Pain and Therapy*, 2017, **6**, 35.
8 T. P. Snutch, *NeuroRx*, 2005, **2**, 662.
9 P. Beswick, 7.03 – Progress in the Discovery of Ca Channel Blockers for the Treatment of Pain A2 – Chackalamannil, Samuel, in *Comprehensive Medicinal Chemistry III*, ed. D. Rotella and S. E. Ward, Elsevier, Oxford, 2017, pp. 65–130.
10 R. Patel, C. Montagut-Bordas and A. H. Dickenson, *Br. J. Pharmacol.*, 2018, **175**, 2173.
11 **https://www.biospace.com/article/releases/persica-pharmaceuticals-completes-recruitment-into-modic-trial-assessing-efficacy-of-pp353-to-treat-chronic-lower-back-pain/**, viewed 5th June 2024.
12 **https://staybletherapeutics.com/research/**, viewed 5th June 2024.
13 P. J. Duggan and K. L. Tuck, *Toxins*, 2015, **7**, 4175.
14 F. C. Cardoso, M.-A. Marliac, C. Geoffroy, M. Schmit, A. Bispat, R. J. Lewis, K. L. Tuck and P. J. Duggan, *Bioorg. Med. Chem.*, 2020, **28**, 115655.
15 T. T. Wager, X. Hou, P. R. Verhoest and A. Villalobos, *ACS Chem. Neurosci.*, 2010, **1**, 435.
16 T. T. Wager, X. Hou, P. R. Verhoest and A. Villalobos, *ACS Chem. Neurosci.*, 2016, **7**, 767.
17 A. S. Bispat, F. C. Cardoso, M. M. Hasan, Y. Dongol, R. Wilcox, R. J. Lewis, P. J. Duggan and K. L. Tuck, *RSC Med. Chem.*, 2024, **15**, 916.
18 S. Gao, X. Yao and N. Yan, *Nature*, 2021, **596**, 143.
19 Y. Zhao, G. Huang, J. Wu, Q. Wu, S. Gao, Z. Yan, J. Lei and N. Yan, *Cell*, 2019, **177**, 1495.
20 *Schrödinger Release 2020–3: Maestro*, Schrödinger, LLC, New York, NY, 2021.
21 J. R. McArthur, L. Motin, E. C. Gleeson, S. Spiller, R. J. Lewis, P. J. Duggan, K. L. Tuck and D. J. Adams, *Br. J. Pharmacol.*, 2018, **175**, 2284.

Open Access Article. Published on 12 June 2024. Downloaded on 2/3/2026 11:10:36 AM.
This article is licensed under a Creative Commons Attribution-NonCommercial 3.0 Unported Licence.

22 S. Hering, E. M. Zangerl-Plessl, S. Beyl, A. Hohaus, S. Andranovits and E. N. Timin, *Pflugers Arch.*, 2018, **470**, 1291.
23 S. Beyl, P. Kügler, M. Kudrnac, A. Hohaus, S. Hering and E. Timin, *J. Gen. Physiol.*, 2009, **134**, 231.
24 D. Pedersen and C. Rosenbohm, *Synthesis*, 2001, **16**, 2431.
25 H. Fukuda, F. Karaki, K. Dodo, T. Noguchi-Yachide, M. Ishikawa, Y. Hashimoto and K. Ohgane, *Bioorg. Med. Chem. Lett.*, 2017, **27**, 2781.
26 W. Humphrey, A. Dalke and K. Schulten, *J. Mol. Graphics*, 1996, **14**, 33.

 This journal is © The Royal Society of Chemistry 2024